Effect of the Preparation Conditions on the Permeation of Ultrahigh-Molecular-Weight Polyethylene/Silicon Dioxide Hybrid Membranes

Nana Li, Changfa Xiao

Key Laboratory of Hollow Fiber Membrane Material and Process of Ministry of Education, Tianjin Polytechnic University, Tianjin 300160, China

Received 4 August 2009; accepted 7 January 2010
DOI 10.1002/app.32073
Published online 27 April 2010 in Wiley InterScience (www.interscience.wiley.com).

ABSTRACT: Porous ultrahigh-molecular-weight polyethylene/SiO_2 membranes were prepared by thermally induced phase separation (TIPS) with white mineral oil as the diluent and SiO_2 as an additive. Influential factors, including extraction method, SiO_2 content, and cooling rate, were investigated. The results suggest that the both porosity and pure water flux of the membranes by extraction of the solvent naphtha in the tension state with alcohol were the best among our research. With increasing SiO_2 content, the porosity, pure water flux, and pore diameter increased. However, with excessive SiO_2 content, defects formed easily. Moreover, SiO_2 improved the pressure resistance of the membranes. The cooling rate directly effected the crystal structure. A slow cooling rate was good for crystal growth and the integration of the diluent. Therefore, the porosity, pure water flux, and bubble-point pore diameter increased with decreasing cooling rate. © 2010 Wiley Periodicals, Inc. J Appl Polym Sci 117: 2817–2824, 2010

Key words: high performance polymers; membranes; microstructure; polyethylene (PE)

INTRODUCTION

Membrane materials are an important part of membrane separation technology. With the development of membrane technology, the requirement should be higher for the performance of membrane materials, including chemical stability, mechanical intensity, and so on, in industry. As a new type of engineering thermoplastic applied in membrane technologies, ultrahigh-molecular-weight polyethylene (UHMWPE) has been widely used in bearing applications because of its good chemical stability, biocompatibility, and friction-reducing and antiwear abilities.[1,2] It has also been used in some components or parts of machines in chemical engineering, textile engineering, transportation engineering, agricultural engineering, food processing, and paper making because of its excellent chemical-corrosion resistance, water-repellent functionality, poor adhesion to polymer matrices, and self-lubricity.[3] However, UHMWPE presents a rubbery state in melting because of its ultrahigh-molecular-weight (more than 1.0×10^6). Thus, UHMWPE almost has no liquidity. Furthermore, UHMWPE has a small frictional coefficient and a low critical shearing rate. All of these make UHMWPE hard to process. Thereby, it is seldom made into membranes with routine method such as melt stretching.

The thermally induced phase separation (TIPS) method was first used by Castro[4] in the 1980s and has gained much interest. It is a valuable method for producing microporous structures in some applications.[5,6] In the TIPS process, polymer and diluent are blended to a homogeneous phase at a sufficiently high temperature. The diluent is a low-molecular-weight, high-boiling chemical that is not a solvent for the polymer at room temperature but acts as one at higher temperatures. The homogeneous solution undergoes phase separation with the diluent extracted when it is cooled. The diluent is then extracted. The voids left by the droplets are referred to as *cells*.[7,8] The viscosity of the UHMWPE/diluent system is smaller than that of the UHMWPE melt. Therefore, microporous membranes of UHMWPE can be prepared by TIPS. Lopatin and Yen[9] first prepared microporous membranes of UHMWPE by the TIPS method, using mineral oil as the diluent. Both the air permeability and water permeability of the UHMWPE membranes were better than those of high-density polyethylene membranes. The porosity was 64% when the extractant was hexane, whereas it was 48% when the extractant was ethanol. Takia

Correspondence to: C. Xiao (xiaocf@yahoo.cn).
Contract grant sponsor: National Basic Research Program (also called 863 Program); contract grant number: 2007AA030304.
Contract grant sponsor: Ministry of Science and Technology of China.

et al.[10] investigated different UHMWPE/high-density polyethylene blending ratios and discovered that the elongation of the membrane increased and the thermal shrinkage of the membrane decreased with increasing UHMWPE. Porous membranes of UHMWPE were prepared as thermally resistant and solvent-resistant membranes by the thermally TIPS method by Ding et al.[11] in 2007. Diphenyl ether and decalin were chosen as the diluents. The phase diagrams were drawn with the cloud-point temperatures and the crystallization temperatures. The influential factors, including the polymer concentration, cooling rate, and viscosity, were investigated. Yu et al.[12] studied nano-SiO_2 dispersed in nanosize in a UHMWPE solution. The results showed that the crystallinity decreased and the crystal grain size increased with increasing nano-SiO_2 concentration. Chen et al.[13] added nanosized SiO_2 into poly(vinylidene fluoride) casting solutions, and the resulting suspensions were uniform, transparent, and stable. The addition of nanosized SiO_2 increased the viscosity of the casting solution and slowed the coagulation process. The results showed that flux and porosity increased, the retention of BSA decreased slightly, and the contact angle decreased.[13] In Zuo et al.'s[14] study, a new type of inorganic–organic anion-exchange membrane based on poly(vinylidene fluoride) was prepared with different weight fractions of SiO_2 nanoparticles. In his study, the effect of SiO_2 content on the performance of these anion-exchange membranes was characterized extensively in terms of the transport properties (TSPs), such as ion-exchange capacity, membrane conductivity, and water content, of anion-exchange membranes. Higher TSP values of these membranes were obtained, which increased with increasing SiO_2 content. The hydrophilic properties of the membranes improved in the presence of SiO_2, which was supported by the observations made on the basis of the obtained increased water uptake and porosity. These anion-exchange membranes prepared with a 2% loading of nanoparticles exhibited better TSPs and may be used for application in electrodriven separation or for other electrochemical processes. In the previous studies, nanosized SiO_2 was only used to control the process of membrane formation and improve the hydrophilicity; electrochemical, thermal, and electrical properties; and mechanical, chemical, and dimensional stabilities of the membrane. In this study, the research objective was to increase the porosity of the membrane by the production of an interface microviod.[15]

In this study, microsized SiO_2 was chosen as the additive. The objective of adding microsized SiO_2 was to increase the interface size between SiO_2 and UHMWPE because of the phase separation that occurs in incompatible UHMWPE/SiO_2 blends. The larger the interface size was, the more easily the stress concentration occurred. Therefore, microsized SiO_2 benefited the formation of interface microvoids. However, it was rare that building an interface microvoid between UHMWPE and SiO_2 by means of adding a mass of micrometer-sized SiO_2 into the UHMWPE solution.

The objective of this study was to obtain a UHMWPE/SiO_2 hybrid membrane with a higher porosity and excellent permeability. Moreover, influential factors, including the extraction method, SiO_2 weight fraction, and cooling rate, were investigated through control of the crystal grain size and interface microvoid.

EXPERIMENTAL

Materials

The UHMWPE (MIII) was purchased from Beijing No. 2 Reagent Plant (Beijing, China) with a weight-average molecular weight of 3.65×10^6 g/mol. No. 7 white mineral oil and the solvent naphtha 120 (surface tension of naphtha $= 2.9 \times 10^{-4}$ J/cm^2) were produced by the Oil Refinery Plant of Daqing Petrochemical Co. (Heilongjiang, China). The white mineral oil was a blends of C16–C31 normal and isomeric alkenes. The kinematic viscosity at 40°C was 7.5–9.0 m^2/s. The molecular weight was 250–450. The main components of the solvent naphtha 120 were aliphatic compounds. It was inflammable and nontoxic. The antioxidant 1076 [*n*-octadecyl-β-(4-hydroxyl-3,5-di-*tert*-butylphenyl) propionate] was a commercial product of Tianjin Lisheng Chemical Plant. It was a white crystalline powder. The microsized SiO_2 (2–6 μm) was kindly provided by Tianjin Chemical Research Institute. Poly(ethylene glycol) (PEG) with a weight-average molecular weight of 20,000 (PEG20000), alcohol (surface tension of alcohol $= 2.2 \times 10^{-4}$ J/cm^2), and glycerol were analytically pure.

Preparation of the UHMWPE/SiO_2 hybrid membranes

The steps for preparing the porous UHMWPE/SiO_2 hybrid membranes were as follows. First, diluent and SiO_2 were mixed well at 50°C at high rotating speed (45 rpm) in a stirred autoclave for 1 h. Then, UHMWPE and the antioxidant were dissolved in a mixture of the diluent and SiO_2 and heated to 140°C for 1 h. The mass ratio of UHMWPE to the diluent was 5/94.7, and the mass ratio of antioxidant to diluent was 0.3/94.7. The mass ratio of SiO_2 to UHMWPE is shown in Table I. After swelling for 1 h, the solution was stirred strongly for 3–4 h at 175°C to prepare the homogeneous casting solution. All of the previous steps were performed *in vacuo* to prevent bubbles in the solution. The resulting homogeneous solution was cast onto a steel plate to form a flat gel membrane by immersion in a cooling medium, which was 20°C water. Different temperatures were used to determine the effect of the cooling rate

TABLE I
Weight Ratios of SiO_2 and UHMWPE in the Casting Solution

Sample	Weight ratio of SiO_2 to UHMWPE
1#	0 : 5
2#	1 : 5
3#	2 : 5
4#	3 : 5
5#	4 : 5
6#	5 : 5
7#	6 : 5

on the permeability of the membranes. The gel membranes were put into the solvent naphtha for 48 h to extract the diluent, and the last step was to take some measures to extract the solvent naphtha.

We used four methods to extract the solvent naphtha in this study. Direct extraction of the solvent naphtha in a relaxed state with alcohol was extraction method I. Direct extraction of the solvent naphtha in a tension state with alcohol was extraction method II. Extraction of the residual solvent naphtha in a relaxed state with alcohol after volatilization of the solvent naphtha in air for 12 h was extraction method III. Extraction of the residual solvent naphtha in a tension state with alcohol after volatilization of the solvent naphtha in air for 12 h was extraction method IV. When we studied the effect of the SiO_2 content and cooling rate on the permeability of the membranes, we used extraction method IV. The resulting membranes were washed with fresh water. Before the scanning electron microscopy (SEM) test, we put the resulting membranes in a glycerol–water solution (3 parts glycerol to 2 parts water) for 24 h and then dried them in air, in which the porous structure was retained.

Pure water flux experiment

The membranes were kept in fresh water for at least 48 h. The pure water flux (J) of the UHMWPE/SiO_2 hybrid membranes was calculated by eq. (1):[16]

$$J = \frac{V}{St} \tag{1}$$

where V is the total permeation (L), S is the total permeation area (m^2), and t is the total permeation time (h). The operating pressure difference across the membrane was 0.1 MPa, and the operating temperature was 25 ± 1°C.

Pressure-resistance measurement

The pressure resistance of the membranes was characterized by the decay rate of pure water flux. The membranes were operated for 480 min. The decay rate of pure water flux was defined as follows:

$$R_{PWF}(\%) = \left(1 - \frac{J_n}{J_0}\right) \times 100 \tag{2}$$

where J_0 is the original pure water flux of the membrane and J_n is the pure water flux of the membrane after operating for n min.

Porosity measurement

The porosity of the blend membrane was determined with the true density and the bulk density.[17] The sample was put into a density bottle (10 mL) filled with alcohol, and the equation of cubage was expressed as

$$10 = \frac{M_a}{\rho_a} + \frac{M_m}{\rho_t} \tag{3}$$

where M_a and M_m are the weights of residual alcohol in the density bottle and dry membrane, respectively; ρ_a is the density of alcohol, and ρ_t is the true density of the membrane. Therefore, ρ_t was calculated according to eq. (4):

$$\rho_t = \frac{M_m \rho_a}{10\rho_a - M_a} \tag{4}$$

To measure the bulk density, the blend membrane was swollen at 20°C for 12 h, and the wet weight (M_{wm}) was measured. The free liquid on the surface of the swollen membrane was padded dry with filter paper before weighing. The dry weight (M_{dm}) was measured after the sample was dried *in vacuo*. The bulk volume (V_b) was calculated by eq. (5):

$$V_b = \frac{M_{wm} - M_{dm}}{\rho_a} + \frac{M_{dm}}{\rho_t} \tag{5}$$

The bulk density (ρ_b) was calculated by eq. (6):

$$\rho_b = \frac{M_{dm}}{V_b} \tag{6}$$

The porosity (ε) of the sample was calculated by eq. (7):

$$\varepsilon(\%) = \left(1 - \frac{\rho_b}{\rho_t}\right) \times 100 \tag{7}$$

Bubble-point pore diameter and pore diameter distribution measurements

The bubble-point pore diameter and pore diameter distribution were measured with the gas permeation method. The membranes were put into the wetting fluid for 2 h and then operated from 0 MPa to

higher pressures in a capillary flow porosimetry system (CFP-1100-A*, Porous Materials, (New York, USA). The bubble-point pore diameter was defined as by Laplace:[18]

$$r = \frac{2\sigma \cos\theta}{\Delta P} \quad (8)$$

where σ is the coefficient of the surface tension of the wetting fluid; θ is the contact angle between the wetting fluid and membrane, which was measured with a contact angle goniometer (JY-820, Chengde Testing Machine Co. (Hebei, China); and ΔP is the operating pressure when the first bubble appears.

The dry flow (F_d) and wet flow (F_w) were measured. The filter flow (F_f) was calculated by eq. (9):

$$F_f(\%) = \frac{F_w}{F_d} \times 100 \quad (9)$$

The pore diameter distribution (PDD) was defined by eq. (9):[19]

$$\mathrm{PDD}(\%) = \frac{F_{f(\mathrm{current})} - F_{f(\mathrm{previous})}}{PD_{(\mathrm{previous})} - PD_{(\mathrm{current})}} \quad (10)$$

where $PD_{(\mathrm{current})}$ is the pore diameter corresponding to the current operation pressure, $PD_{(\mathrm{previous})}$ is the pore diameter corresponding to the previous operation pressure, $F_{f(\mathrm{current})}$ is the filter flow corresponding to the current operation pressure, and $F_{f(\mathrm{previous})}$ is the filter flow corresponding to the previous operation pressure.

Morphological examination

The structure and morphology of membranes were observed by SEM (Quanta 200, FEI, Eindhoven, Netherlands). The cross section of the membranes was freeze-fractured under liquid nitrogen. The membrane samples were gold sputtered and analyzed by SEM.

Wide X-ray diffraction experiment

Wide-angle X-ray diffraction patterns were done on a diffractometer (X'pert MPD, Philips, Eindhoven, Netherlands). The X-ray beam was graphite monochromator-filtered (λ = 1.54 Å) and Cu Kα radiation operating at 40 kV and 45 mA. The scanning speed was 8°/min. The scanning area of the Bragg angle was from 5 to 70°.

The crystal grain size was calculated by the Sherrer equation:[20]

$$D_{hkl} = \frac{K\lambda}{\beta \cos\theta_{hkl}} \quad (11)$$

where θ_{hkl} is the Bragg angle of a certain diffraction plane (*hkl*), λ is the wavelength of the incident wave, D_{hkl} is the average size of the normal direction of the crystal plane, β is the peak width, and K is the Sherrer constant. The value of K was about 0.89 when β was the peak width at half-height.

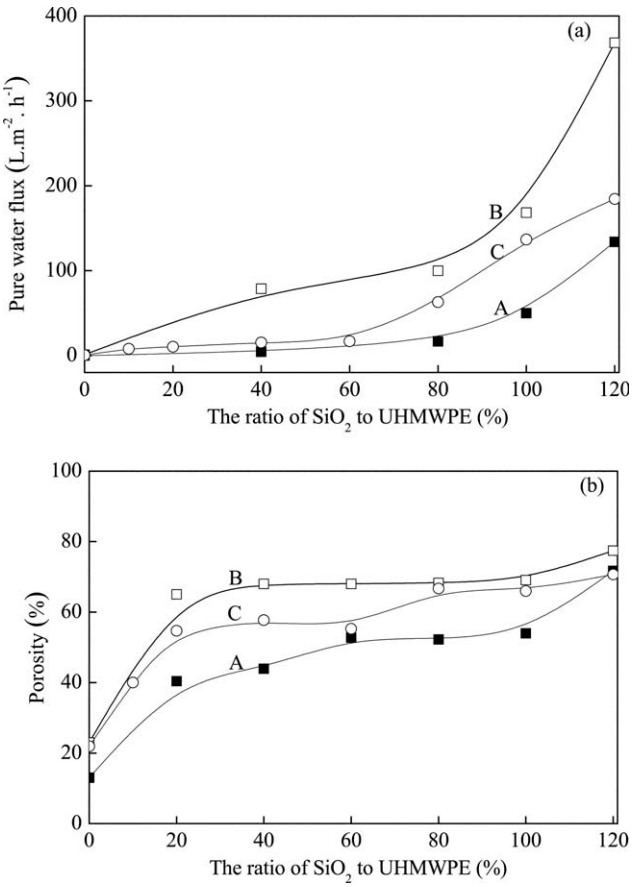

Figure 1 Effect of the extraction method on the permeability of the membranes: extraction methods (A) I, (B) II, and (C) IV.

RESULTS AND DISCUSSION

Effect of the extraction method

Figure 1 displays the effect of the extraction method on the permeability of the membrane. As shown, extraction method II formed membranes with the highest porosity and pure water flux, extraction method IV took second place, and extraction method III was the worst. The pure water flux and porosity data obtained by extraction method III were approximately zero over the range of SiO_2/UHMWPE ratios (data not shown).

This is the result of pore collapse during the drying step due to large capillary forces imposed at the liquid–vapor interface.[21] The collapse happened easily when extraction was taken in the relaxed state and was prevented when extraction was taken in the tension state. There were many tensile pores in the membranes with extraction done in tension, as

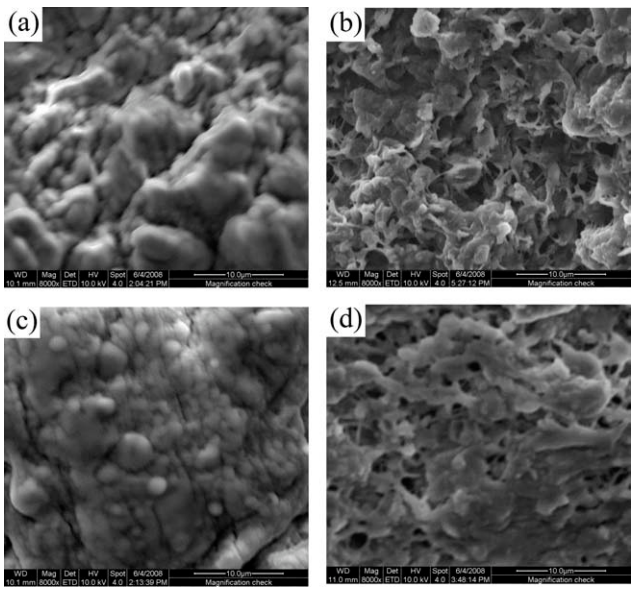

Figure 2 Cross-sectional SEM graphs of 5# membranes through extraction methods (a) I, (b) II, (c) III, and (d) IV.

shown in Figure 2(b,d). However, the dense pore structure was formed by membrane shrinkage when the extraction was done under the relaxed state [Fig. 2(a,c)]. In this case, the porosity and pure water flux were small.

As shown in Figure 3 and Table II, the diffraction peaks at 20.98 and 23.36° in extraction methods II and IV were orthorhombic (110) and (200) reflections.[22] The crystal grain sizes of the membrane obtained by extraction method II were greater than that of the membrane obtained by extraction method IV. Furthermore, the diffraction peak at 20.0° in extraction method II was the hexagonal (100) reflection. The porosity and pure water flux of the membrane obtained by extraction method IV were lower

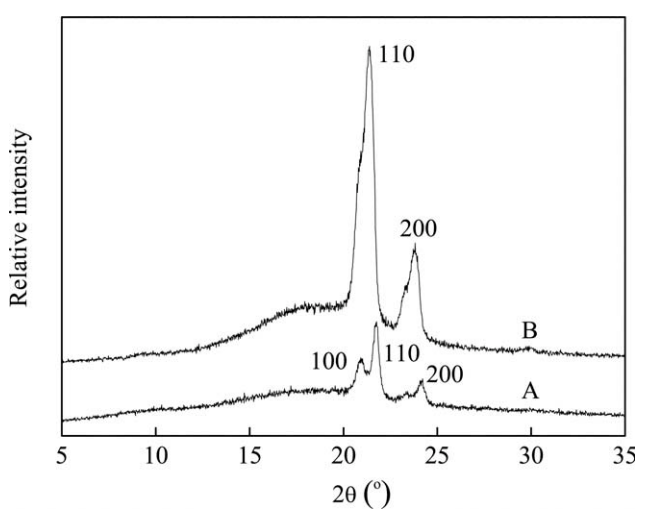

Figure 3 Effect of the extraction method on the X-ray diffraction pattern of the UHMWPE membranes: extraction methods (A) II and (B) IV.

TABLE II
Effect of the Extraction on the Crystal Grain Size in the UHMWPE Membrane

Sample	D_{100} (nm)	D_{110} (nm)	D_{200} (nm)
Extraction method II	12.92	18.47	14.47
Extraction method IV	–	7.84	8.99

D_{100}, D_{110}, D_{200} are the sizes of crystal plane (100), (110), (200), respectively.

than those of the membrane obtained by extraction method II. This was attributed to membranes swelling in alcohol in extraction method II. The swelling action was good for macromolecular motion and reform crystallization. Therefore, the membrane obtained by extraction method II had a higher degree of crystallinity and bigger crystal grains. The pore between the two crystal grains was bigger.

Extraction method II was the best of the four. However, the solvent consumption in extraction method II was too high for practical application. Accordingly, extraction method IV was used mainly in this study.

Effect of the SiO_2 content

As shown in Figures 4 and 5, the pure water flux of the UHMWPE membrane was very low; this was because of the dense pore structure formed by the molecular network [Fig. 6(a)].

With increasing SiO_2 content, the porosity, pure water flux, and pore diameter all increased. This was because of the massive interface microvoid produced by phase separation between UHMWPE and SiO_2, which were incompatible. The number and size of the interface microvoid increased with increasing SiO_2, as shown in Figure 6(b,c). However, the SEM results displayed both permeable pores and impermeable pores. The effective aperture was

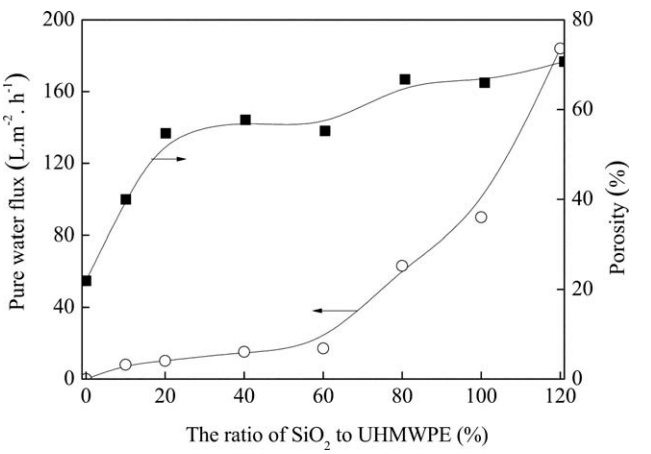

Figure 4 Effect of the SiO_2 content on the permeability of the membranes.

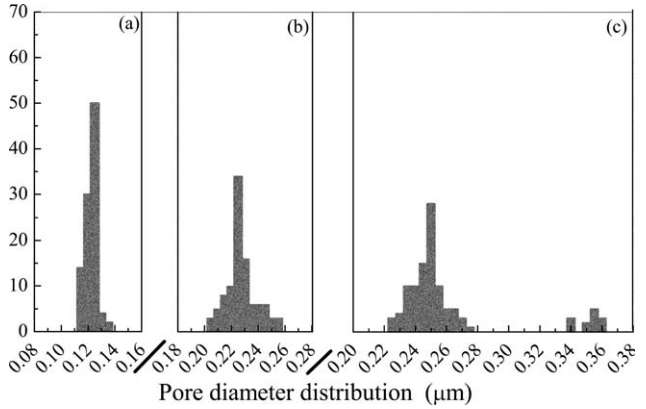

Figure 5 Effect of the SiO_2 content on the pore diameter distribution of the membranes: (a) 3#, (b) 6#, and (c) 7#.

related to the tortuosity of the permeable pores. The effective aperture was measured by a capillary flow porosimetry system.

When the SiO_2 content was too large, excess SiO_2 could not homodisperse but congregated into big particles. As shown in Figure 6(d), the maximum pore diameter reached about 4 μm because of the gap between the two big particles. However, the percentage of big pore diameters was very low, as shown in Figure 5(c). Because the difference between the pore diameter was too large, these maximum pores can be seen as defects. Thus, excessive SiO_2 content is not advisable.

Figure 7 displays the pressure resistance of the membranes. When the additive was PEG20000, the membrane was composed of UHMWPE because of the washing away of PEG. PEG was mainly used to

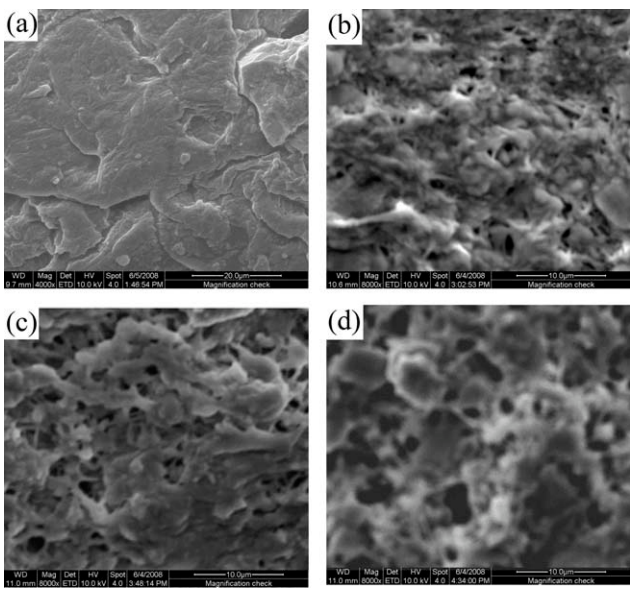

Figure 6 Cross-sectional SEM graphs of (a) 1#, (b) 3#, (c) 5#, and (d) 7# membranes.

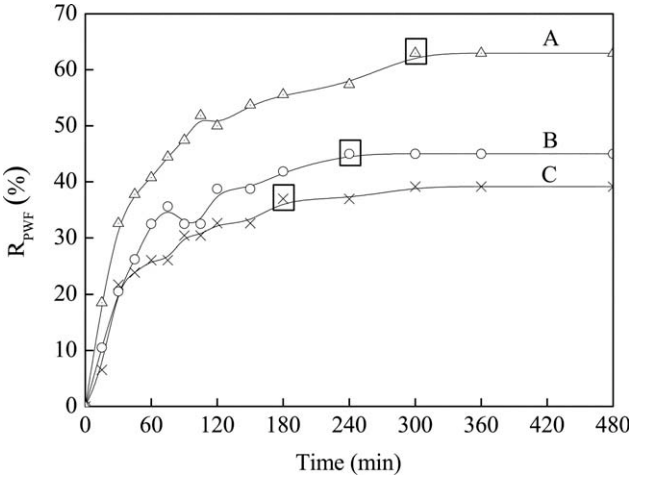

Figure 7 Effect of SiO_2 on the decay rate of pure water flux: (A) UHMWPE/PEG (5%)/white oil, (B) UHMWPE/SiO_2 (5/3)/white oil, and (C) UHMWPE/SiO_2 (5/6)/white oil. (The boxes around the data points are labels of R_{PWF} reaching invariableness.)

increase the pure water flux. As shown, the decadent speed of pure water flux of UHMWPE was very high with time. The decay rate of pure water flux (R_{PWF}) of the UHMWPE membrane reached invariableness at 300 min and was above 60%. Thus, the pressure resistance of the UHMWPE membrane was too bad for practical application. This result was attributed to the low glass-transition temperature of UHMWPE[23] and the loose pore structure coming from PEG20000 dissolution.

When the additive was SiO_2, the decadent speed of pure water flux of UHMWPE/SiO_2 was low with time. R_{PWF} decreased with increasing SiO_2 at the same time. The time for R_{PWF} to reach invariableness was shortened with increasing SiO_2. Accordingly, SiO_2 improved the pressure resistance of the UHMWPE membrane. These trends were due to rigid SiO_2, which played a supporting role in the membrane and the steady pore structure coming from interface microvoids between UHMWPE and SiO_2.

Effect of the cooling rate

As shown in Figure 8, the pure water flux, bubble-point pore diameter, and porosity all increased with the temperature of the cooling medium. These trends were attributed to the effect of the cooling rate on the diluent droplet growth and crystal state.[24–26]

When the cooling rate was high, the viscosity of the diluent became higher before crystallization of the polymer. The density of the crystal nucleus was large, and the crystal grain size was small; this evidently resulted from the polymer crystallization

being hindered by the high viscosity of the diluent. The gap between the two crystallites was very small. Furthermore, at high cooling rates, the time of phase separation before solidification was shortened, and then, the polymer-rich phase and the polymer-lean phase did not have enough time to coarsen. Thus, the diluent could not congregate into a bigger droplet. These made the pore diameter small at high cooling rates, as shown in Figure 9(a). The pore diameter and pure water flux of the membrane were very small at high cooling rates. The results were contrary when the temperature of the cooling medium increased. Also, with the big gap between tow crystallites and the big pore resulting from the extraction of bigger droplets, micelle pores were formed, as shown in Figure 9(b). A slow cooling rate was good for macromolecular chain entanglement, once again at high temperatures. The micelle pores were larger than the molecular network pores. Accordingly, the high temperature of the cooling medium could be used to prepare UHMWPE/SiO$_2$ membranes with better permeabilities.

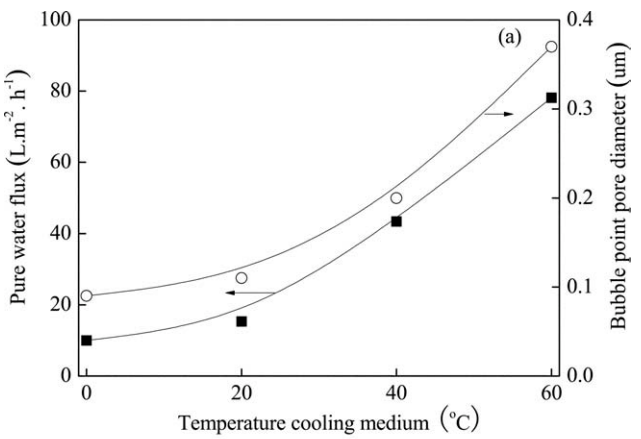

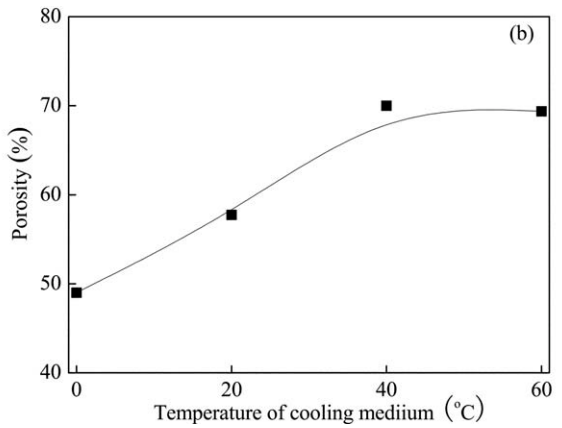

Figure 8 Effect of the temperature of the cooling medium on the permeability of 3# membranes.

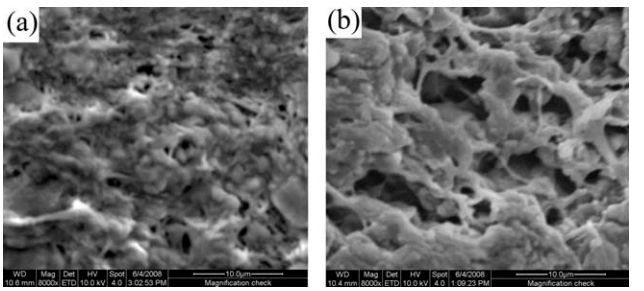

Figure 9 Cross-sectional SEM graphs of 3# membranes in cooling media at (a) 20 and (b) 60°C.

CONCLUSIONS

UHMWPE/SiO$_2$ hybrid membranes were prepared by TIPS with white mineral oil as the diluent. The results of this study indicate that the porosity and pure water flux of the membranes extracted with method II were the best among our research. The pure water flux of the UHMWPE membrane was very low. In the UHMWPE/SiO$_2$ hybrid membranes, there were massive interface microvoids produced by phase separation between UHMWPE and SiO$_2$. This contributed to the improvement of the porosity and pure water flux. With increasing SiO$_2$ content, the porosity, pure water flux, and pore diameter increased. However, excessive SiO$_2$ content was not advisable. Moreover, the pressure resistance of the UHMWPE/SiO$_2$ hybrid membranes was better than that of the UHMWPE membrane. The cooling rate directly influenced the crystal structure. The porosity, pure water flux, and bubble-point pore diameter increased with decreasing cooling rate. Future studies will be aimed at the preparation of UHMWPE/SiO$_2$ hybrid hollow-fiber membranes and the investigation of the barrier properties.

The authors thank Professor Shulin An for his theoretical contributions during the early stages of this study.

References

1. Cohen, Y. D.; Rein, M.; Vaykhansky, L. Compos Sci Technol 1997, 57, 1149.
2. Turell, M. B.; Bellare, A. Biomaterials 2004, 25, 3389.
3. Kurtz, S. M.; Muratoglu, O. K.; Evans, M. Biomaterials 1999, 20, 1659.
4. Castro, A. J. U.S. Pat. 4,247,498 (1981).
5. Lloyd, D. R.; Barlow, J. W.; Kinzer, K. E. Microporous Membrane Formation via Thermally-Induced Phase Separation; American Institute of Chemical Engineers Press: New York, 1988.
6. Kim, J. J.; Hwang, J. R.; Kim, U. Y.; Kim, S. S. J Membr Sci 1995, 108, 25.
7. Lloyd, D. R.; Kinzer, K. E.; Tseng, H. S. J Membr Sci 1990, 52, 239.
8. Lloyd, D. R.; Kim, S. S.; Kinzer, K. E. J Membr Sci 1991, 64, 1.
9. Lopatin, G.; Yen, L. Y. U.S. Pat. 4,778,601 (1988).
10. Takia, K.; Funaoka, H.; Kaimai, N. U.S. Pat. 6,245,272 (2001).

11. Ding, H. Y.; Tian, Y.; Wang, L. H. J Appl Polym Sci 2007, 105, 3355.
12. Yu, J. R.; Hu, Z. M.; Liu, Z. F. J Donghua Univ 2005, 31, 1.
13. Chen, N.; Peng, Y. L.; Ji, S. L. Membr Sci Tech 2007, 27, 21.
14. Zuo, X. T.; Yu, S. L.; Xu, X.; Xu, J. J Membr Sci 2009, 340, 206.
15. Samuels, R. J. J Polym Sci Polym Phys Ed 1979, 17, 535.
16. Wang, Z. Foundation of Membrane Separation Technology; Chemical Industry Press: Beijing, 2000.
17. Kim, J. H.; Min, B. R.; Park, H. C.; Won, J.; Kang, Y. S. J Appl Polym Sci 2001, 81, 3481.
18. Chen, T. Y.; Chiu, M. S.; Weng, C. N. J Appl Phys 2006, 100, 1.
19. Chiu, H. C.; Huang, J. J.; Liu, C. H.; Suen, S. Y. React Funct Polym 2006, 66, 1515.
20. Smook, J.; Pennings, J. Colloid Pol Sci 1984, 262, 712.
21. Brinker, C. J.; Scherer, G. W. J Non-Cryst Solids 1985, 70, 301.
22. Xiao, C. F.; An, S. L.; Jia, G. X.; Zhang, Y. Z. Acta Polym Sinica 1999, 2, 171.
23. Kavesh, S.; Prevorsek, D. C. Int J Polym Mater 1995, 30, 15.
24. Masuyama, H.; Teramoto, M.; Kllwamllra, M. Polym 2000, 41, 8673.
25. Kim, S. S.; Lloyd, D. R. J Membr Sci 1991, 64, 13.
26. Matsuyama, H.; Kim, M. M.; Lloyd, D. R. J Membr Sci 2002, 204, 413.